Optical and magnetic properties of Mn in bulk GaN

A. Wolos

Institute of Experimental Physics, Warsaw University, Hoza 69, 00-681 Warsaw, Poland

M. Palczewska

Institute of Electronic Materials Technology, Wolczynska 133, 01-919 Warsaw, Poland

M. Zajac

Institute of Experimental Physics, Warsaw University, Hoza 69, 00-681 Warsaw, Poland

J. Gosk

Institute of Experimental Physics, Warsaw University, Hoza 69, 00-681 Warsaw, Poland
and Faculty of Physics, Warsaw University of Technology, Koszykowa 75, 00-661 Warsaw, Poland

M. Kaminska and A. Twardowski

Institute of Experimental Physics, Warsaw University, Hoza 69, 00-681 Warsaw, Poland

M. Bockowski, I. Grzegory, and S. Porowski

High Pressure Research Center, Polish Academy of Science, Sokolowska 29/37, 01-142 Warsaw, Poland
(Received 28 July 2003; published 19 March 2004)

We report results of electron paramagnetic resonance, magnetization, and optical absorption studies of bulk GaN crystals doped with Mn and, for some samples, codoped with Mg acceptor. The experiments performed show that the charge state of the Mn ion in GaN depends on the Fermi level position in the crystal. In n-type samples Mn stays as an ionized acceptor A^- center of $Mn^{2+}(d^5)$, while in the investigated highly resistive samples with lowered Fermi level, in a different charge state, most probably corresponding to neutral configuration A^0. Optical absorption spectra of GaN:Mn and GaN:Mn,Mg show characteristic absorption bands related to Mn, which may be interpreted as resulting from photoionization of $Mn^{2+}(d^5)$ to GaN conduction band (in n-type samples) and photoionization of neutral Mn A^0 to GaN valence band (in highly resistive samples). The absorption spectra are discussed in terms of a configuration coordinate model. The location of the Mn acceptor level is derived as 1.8 eV below the bottom of the GaN conduction band. The magnetization experiments performed reveal Brillouin-type magnetization with Mn spin $S=5/2$ in n-type crystals, while the investigated highly resistive samples show magnetic anisotropy characteristic for nonspherical transition-metal configurations. The nature of the Mn ion in GaN is discussed.

I. INTRODUCTION

Theoretical predictions of room-temperature ferromagnetism in GaMnN (Ref. 1) and resulting possible applications in modern electronics have motivated investigations of Mn impurities in GaN. Successful growth of GaMnN epitaxial layers[2–6] as well as microcrystalline powders[7,8] and finally bulk GaN:Mn crystals[9] has been already reported, showing that doping of GaN with Mn is possible up to a few molar percent. The magnetic properties of GaMnN seem to depend on the growth method. Bulk crystals and microcrystals obtained by ammonothermal synthesis show paramagnetic behavior with antiferromagnetic d-d interactions for high Mn content,[7,8] while some epitaxial layers reveal a ferromagnetic response with Curie temperature far above 300 K.[2–6] Some authors relate this ferromagnetism to GaMnN, while others to precipitates of Mn compounds.[10] The nature of the magnetic interactions in GaMnN and, especially, the origin of possible ferromagnetism are still under discussion. A number of competing theoretical models for GaMnN were developed,[1,11–18] among which the most widely discussed is the hole-mediated (Zener) model of ferromagnetism.[1,17,18]

In order to understand the ferromagnetic properties of GaMnN, the nature of the Mn ion in GaN needs to be clarified, as only then will it be possible to verify the assumptions of the proposed theoretical approaches. Especially important for the problem, apart from exchange interactions, are possible electron configurations of Mn and the corresponding energy levels.

The most common configuration of Mn in III-V semiconductors is an ionized acceptor $Mn^{2+}(d^5)$ (denoted as an A^- center), with five tightly bound electrons on the Mn d shell.[19,20] The neutral configuration of Mn (A^0 center) may be realized in two ways, as $Mn^{3+}(d^4)$ with four electrons localized on the Mn d shell[21] or as a $Mn^{2+}(d^5)$+hole with five electrons on the Mn d shell and a band hole weakly bound on a delocalized orbit.[22] The $Mn^{3+}(d^4)$ configuration was reported for wide-band-gap GaP:Mn, for which Mn forms a deep-gap acceptor level,[21] while $Mn^{2+}(d^5)$+hole is a neutral acceptor configuration in GaAs:Mn or InP:Mn, for which the Mn acceptor level is a shallow one.[22–25]

As was discussed, the binding energies of transition-metal
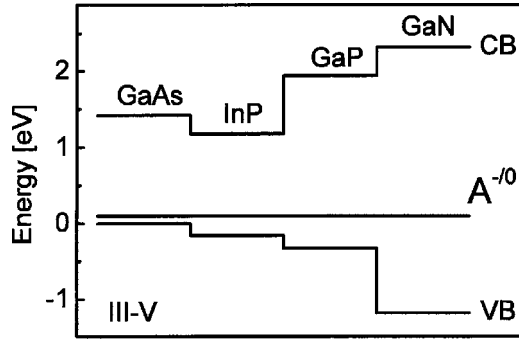
FIG. 1. Band offsets (Refs. 27 and 28) and location of Mn acceptor level $A^{-/0}$ in GaAs, InP, GaP (Refs. 21, 23, and 25) and GaN.

FIG. 2. Electron paramagnetic resonance of $Mn^{2+}(d^5)$ in GaN recorded in the **B**$\|c$ configuration for n-type GaN:Mn with x_{Mn} $=0.01\%$ and for highly resistive GaN:Mn,Mg with $x_{Mn}=0.009\%$. A low EPR amplitude for GaN:Mn,Mg indicates mixed valence of Mn in highly resistive samples.

impurities related to the universal reference level remain constant within a class of III-V (or II-VI) semiconductor compounds.[26,27] Thus comparing the known location of Mn acceptor level $A^{-/0}$ in GaAs, InP, and GaP one may expect that the $A^{-/0}$ level in GaN should be placed deep within its band gap (see Fig. 1). This assertion was primarily corroborated by optical absorption experiments, in which optical transitions to a deep Mn acceptor level have been observed.[9,29–31]

In this communication we report the results of studies of bulk GaN crystals doped with Mn and for some samples codoped with Mg, performed by means of electron paramagnetic resonance (EPR), magnetization, and optical absorption experiments. The aim of the work is to compare the physical properties of GaN:Mn crystals arising from different electron configurations of Mn.

We investigated two kinds of crystals: n-type GaN:Mn, where the high concentration of free electrons is due to the presence of an oxygen residual donor,[32,33] and highly resistive GaN:Mn,Mg samples, where codoping with a Mg acceptor resulted in a lowering of the Fermi level. In the n-type GaN:Mn crystals we expect Mn to be in a $Mn^{2+}(d^5)$ configuration, while in GaN:Mn,Mg neutral Mn acceptor A^0 should appear. We focused on samples with low Mn content, which allowed us to neglect Mn-Mn interactions, and then to study the properties of isolated Mn ions.

II. SAMPLES

The investigated bulk GaN:Mn and GaN:Mn,Mg samples were synthesized from solution of nitrogen in liquid gallium under high pressure of N_2 ($p \approx 1.5$ GPa) and at elevated temperatures $T \approx 1500\,°C$.[32] Doping was obtained by adding Mn and Mg to the melt of gallium. The crystals were platelets with diameter of about a few millimeters and thickness of about $100\ \mu m$, with wurzite structure and c axis perpendicular to the crystal plane. GaN:Mn samples were conductive with a concentration of free electrons $n \approx 10^{19}$ cm^{-3}, whereas GaN:Mn,Mg crystals were highly resistive with $\rho \sim 10^9 \Omega$ cm at room temperature. The content of Mn was evaluated by secondary ion mass spectroscopy (SIMS) and ranged from 0.0005 to 0.2 mol. % depending on the growth conditions.
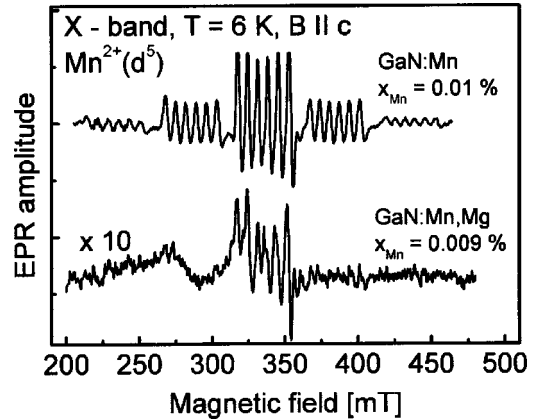
III. ELECTRON PARAMAGNETIC RESONANCE EXPERIMENT

The electron paramagnetic resonance technique is able to provide evidence for the presence of a $Mn^{2+}(d^5)$ charge state in a sample, as this configuration is known as a paramagnetic center with g factor equal 1.999.[19,20,34,35] The neutral Mn configurations are less commonly present in semiconductors. A hydrogen like $Mn^{2+}(d^5)$+hole was detected by EPR in GaAs as two resonant lines, originating from the splitting of the $Mn^{2+}(d^5)$+hole ground state of total angular momentum $J=1$.[22] The $Mn^{3+}(d^4)$-related EPR resonance was observed for GaP in a high magnetic field.[21] In all the investigated bulk GaN:Mn or GaN:Mn,Mg samples we recorded $Mn^{2+}(d^5)$ resonance only.

The investigated samples were characterized by EPR using a Bruker spectrometer operating at a microwave frequency 9.4 GHz (X-band) with magnetic field up to 1 T. Spectra were recorded at $T=6$ K.

The EPR experiment showed a resonance, originating from a manganese-occupying gallium site in the $Mn^{2+}(d^5)$ configuration, in all the n-type GaN:Mn samples. The intensity of the resonant line increased linearly with an increase of Mn concentration in the crystal. Figure 2 shows a classical EPR spectrum related to $Mn^{2+}(d^5)$ resonance recorded in the **B**$\|c$ configuration. The five groups of lines originate from the $\Delta M_S = 1$ transition of the electron system with spin $S=5/2$. Each group is split into six components, due to the interaction with the Mn nucleus having nuclear spin $I=5/2$ (transitions with $\Delta M_I = 0$).

The case of highly resistive GaN:Mn,Mg crystals is quite different. The resonance resulting from substitutional $Mn^{2+}(d^5)$ is very weak for those samples. Figure 2 compares the intensity of the $Mn^{2+}(d^5)$ line, recorded for GaN:Mn and GaN:Mn,Mg samples having similar Mn concentration. The $Mn^{2+}(d^5)$ resonant line is about 10 times weaker in GaN:Mn,Mg, which points to a mixed valence of Mn in the highly resistive sample. In terms of the manganese acceptor level, this means that the Fermi level is placed in
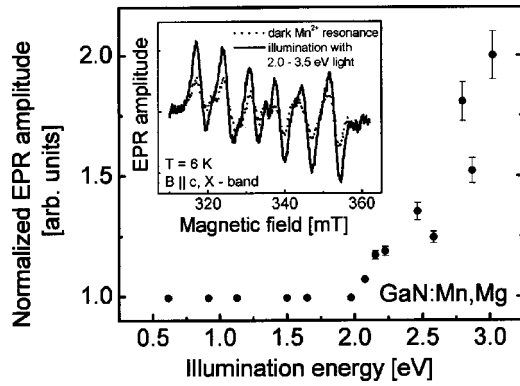
FIG. 3. A photo-EPR experiment performed for a highly resistive GaN:Mn,Mg sample. Spectral dependence of the photostimulated $Mn^{2+}(d^5)$ amplitude is shown. Inset: Dotted line represents the dark EPR signal of $Mn^{2+}(d^5)$, solid line represents a photostimulated signal. An increase of the signal amplitude by a factor of 2 after illumination is evident.

this sample close to $A^{-/0}$. The mixed valence observation in bulk GaN:Mn,Mg is consistent with investigations performed for GaN:Mn epitaxial films, for which the difference in total Mn concentration and $Mn^{2+}(d^5)$ concentration was removed by codoping with a Si donor.[31]

In order to clarify the situation, a photo-EPR experiment was performed for a GaN:Mn,Mg sample containing about 0.009% of Mn. The results are shown in Fig. 3. The dotted line in the inset of Fig. 3 represents a signal related to the $Mn^{2+}(d^5)$ substitutional center in the $\mathbf{B}\|c$ configuration, recorded after cooling the sample in the dark. The solid line represents a photostimulated signal recorded during illumination with light in the energy range 2.0–3.5 eV. An increase of the signal intensity by a factor of 2 under illumination is apparent.

The increase of the EPR amplitude after illumination may be caused either by photoionization of Mn leading to an increase of the $Mn^{2+}(d^5)$ concentration or by a change of the spin relaxation rate. However, the spin relaxation time T_1, determined by the standard method from the $Mn^{2+}(d^5)$ EPR amplitude measured versus microwave power,[36] equals 3.9×10^{-3} s independently of illumination. This shows that the observed increase of the $Mn^{2+}(d^5)$ EPR amplitude in GaN:Mn,Mg after illumination is due to photoionization of Mn.

The spectral dependence of the photo stimulated EPR signal—namely, the amplitude of $Mn^{2+}(d^5)$ resonance versus the energy of light illuminating the sample—is shown in Fig. 3. Data were normalized to the intensity of halogen lamp light and transmission of interference filters used in the experiment. The photoionization spectrum presented in Fig. 3 clearly shows an onset at about 2 eV. We interpret this onset as resulting from direct photoionization of the neutral Mn to GaN valence bands, similarly to the origin of the absorption bands observed in optical absorption spectra of highly resistive GaN:Mn,Mg (see Sec. V), as well as of highly resistive GaN:Mn epitaxial layers.[30] The electron transition discussed may be described as

$$A^0 + h\nu \rightarrow Mn^{2+}(d^5) + \text{hole}_{VB}. \qquad (1)$$
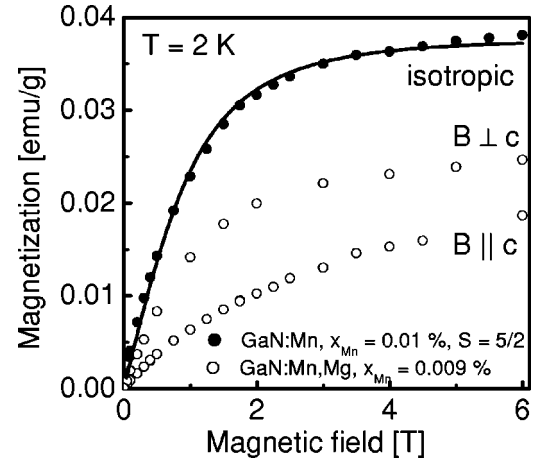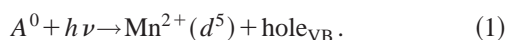
FIG. 4. Magnetic properties of GaN:Mn and GaN:Mn,Mg. Solid circles: Brillouin-type isotropic magnetization of n-type GaN:Mn sample measured as a function of magnetic field at $T = 2$ K. Solid line represents a Brillouin function fit with $S = 5/2$ and $x_{Mn} = 0.01\%$. Open circles: magnetic anisotropy of highly resistive GaN:Mn,Mg with $x_{Mn} = 0.009\%$, originating from the anisotropy of the neutral A^0 center.

The observation of Mn photoionization in our EPR experiment was possible due to metastability of the photostimulated $Mn^{2+}(d^5)$ center in highly resistive GaN:Mn,Mg samples. This metastability was removed after heating the sample up to about 250 K. At this temperature, deep traps having activation energy about 0.3 eV are ionized (compare with deep-level transient spectroscopy spectra, e.g., in Ref. 37). The energy of about 0.3 eV determines thus a barrier height for thermalization of photostimulated $Mn^{2+}(d^5)$. The origin of this barrier will be discussed in Sec. V.

IV. MAGNETIC CHARACTERIZATION

Magnetization measurements were performed by a superconducting quantum interference device (SQUID) magnetometer at magnetic field up to 6 T. All the data were corrected for diamagnetism of the host crystal lattice.

The investigated GaN:Mn bulk crystals exhibit typical Brillouin-type paramagnetism. An insignificant, less than 1%, ferromagnetic contribution to magnetization was also observed in some samples and was attributed to the presence of Mn compound precipitates.[10] Figure 4 (solid circles) shows magnetization versus magnetic field measured for a representative GaN:Mn sample at $T = 2$ K. Together with the experimental data a Brillouin function fit is presented (solid line). The spin of Mn ions was assumed as $S = 5/2$, as indicated by the EPR measurements, and the Mn concentration x_{Mn} was the only fitting parameter. The fit reproduces well the character of the experimental data and the x_{Mn} value obtained agrees reasonably well with the one from SIMS analysis for all measured samples. The observed magnetization was isotropic. Magnetic measurements show consistency with the EPR experiment, giving evidence for a $Mn^{2+}(d^5)$, $S = 5/2$ configuration of Mn ions in the investigated n-type GaN:Mn.

The magnetization of GaN:Mn,Mg samples, in contrast to
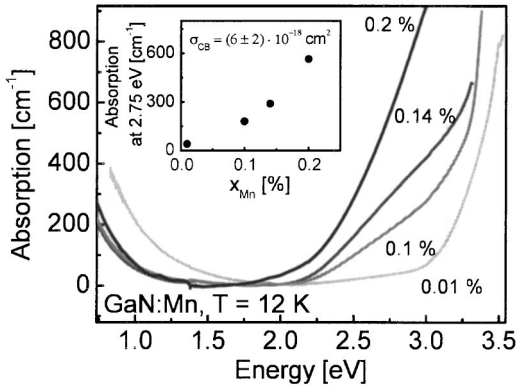
FIG. 5. Optical absorption spectra of n-type GaN:Mn samples showing photoionization of $Mn^{2+}(d^5)$ to the GaN conduction band in the high-energy spectral region. Free-carrier absorption is visible for energies below 1.5 eV. Numbers indicate Mn concentration in a sample. Inset: absorption coefficient at 2.75 eV versus Mn concentration measured for different samples. The optical cross section at 2.75 eV equals $\sigma_{CB}=(6\pm2)\times10^{-18}$ cm^2.

GaN:Mn, shows large magnetic anisotropy. Figure 4 (open circles) presents magnetization versus magnetic field of a GaN:Mn,Mg sample, measured in configurations **B** parallel and perpendicular to the c axis of the GaN crystal.

Magnetic anisotropy is characteristic for nonspherical transition-metal configurations and was observed, e.g., for CdS:Cr$^{2+}(d^4)$ or CdS:V$^{2+}(d^3)$, where it originated from the influence of the hexagonal crystal field on the distribution of nonequivalent Jahn-Teller transition-metal centers.[38,39] This problem for Mn in GaN will be analyzed in detail elsewhere.

V. OPTICAL ABSORPTION

Optical absorption spectra of GaN:Mn and GaN:Mn,Mg were measured using a double-beam Cary 5 spectrometer in the energy range of 0.5–3.5 eV and at temperatures down to 12 K.

Figure 5 shows the absorption of GaN:Mn samples with different Mn concentrations. Characteristic features appearing at the spectrum are the free-carrier absorption tail in the low-energy region, below ~1.5 eV, and a broad band with an onset at about 2.1 eV, the intensity of which scales with Mn concentration in a sample. The optical cross section measured at 2.75 eV for a set of GaN:Mn with different Mn concentrations equals $\sigma_{CB}=(6\pm2)\times10^{-18}$ cm^2. This low value is typical for the forbidden transition between localized d-state and s-type conduction bands.[40,41] Due to the detected $Mn^{2+}(d^5)$ configuration in the investigated n-type GaN:Mn samples, a relatively low optical cross section, and a typical shape for the photoionization transition, we may attribute the observed band to photoionization from the filled $A^{-/0}$ level to the GaN conduction band. This transition may be described as

$$Mn^{2+}(d^5)+h\nu\rightarrow A^0+e_{CB}. \qquad (2)$$
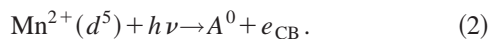
Two other characteristic absorption bands appear at the absorption spectra of highly resistive GaN:Mn,Mg samples
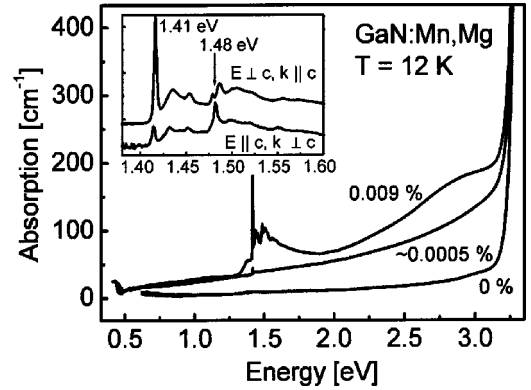
FIG. 6. Optical absorption spectra of highly resistive GaN:Mn,Mg samples. Photoionization of A^0 to the GaN valence band is visible in the high-energy spectral region. Numbers indicate Mn concentration in a sample. Inset: the infrared band related most probably to the internal transition within A^0 configuration, measured at two different sample orientations, is shown in magnification.

(Fig. 6). The band lying in the infrared region consists of two sharp absorption lines at 1.41 eV (observed in $\mathbf{E}\perp c$, $\mathbf{k}\|c$ configurations) and at 1.48 eV (visible in $\mathbf{E}\|c$, $\mathbf{k}\perp c$ configurations) followed by the GaN phonon structures. This infrared band was also observed in highly resistive GaN:Mn epitaxial layers.[29–31] Initially it was attributed to an electron transition from the GaN valence band to the $A^{-/0}$ level,[29] later to an internal transition of A^0 followed probably by thermal ionization to the GaN valence band.[30,31] We incline to the second interpretation, assigning the infrared band to the internal transition within the neutral configuration of Mn.

The absorption band lying in high-energy spectral region, above 2 eV, we assign to the photoionization from the GaN valence band to, partially empty in our samples, the $A^{-/0}$ level. This description is consistent with the interpretation proposed in Refs. 30 and 31. The optical cross section for this absorption is of the order of 2×10^{-17} cm^2 at the band maximum, which is typical for the allowed transitions from the localized d-state to p-type valence band.[40,41]

In the investigated GaN:Mn,Mg samples Mn is in the mixed-valence state: therefore, transitions from the $A^{-/0}$ to GaN conduction band are also present in the high-energy spectral region. However, photoionization to the conduction band is about an order of magnitude weaker than photoionization to the valence band and thus may be neglected for the spectrum presented in Fig. 6.

It is important to note here that the sum of the optical photoionization energies from the GaN valence band to $A^{-/0}$ ($E_{opt}^{VB}\sim2.0$ eV as derived from photo-EPR and optical absorption spectra) and from $A^{-/0}$ to the GaN conduction band ($E_{opt}^{CB}\sim2.1$ eV as derived from optical absorption spectra) is fairly greater than the GaN band gap ($E_g^{GaN}=3.5$ eV). This fact may be interpreted in terms of lattice relaxation during photoionization of Mn. Typical lattice relaxation energies in semiconductors vary from 0.1 to 0.4 eV,[27] depending on the impurity-ligand bond ionicity. For the analyzed case of Mn in GaN we may estimate the relaxation energy on the order of $E_{rel}=0.3$ eV, as approximated by the equation
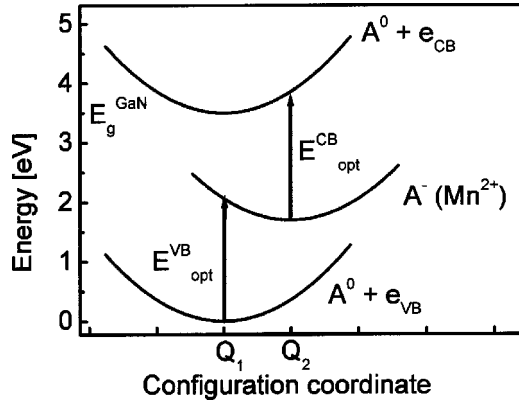
FIG. 7. Configuration-coordinate diagram showing Mn-related optical transitions in GaN. Parabolas represent energy levels. The optical transitions occur without changing the configuration coordinate, at Q_1 with optical energy E_{opt}^{CB} for the $A^0 + h\nu \rightarrow Mn^{2+}(d^5)$ $+ hole_{VB}$ transition and at Q_2 with E_{opt}^{VB} for $Mn^{2+}(d^5) + h\nu \rightarrow A^0$ $+ e_{CB}$. Thermal energies are determined by the minima of configuration parabolas. The relaxation energy is a difference between optical energy and thermal energy for a given transition.

$$E_{rel} \approx \frac{1}{2}(E_g - E_{opt}^{CB} - E_{opt}^{VB}). \qquad (3)$$

In order to describe quantitatively the observed Mn optical transitions in GaN a configuration-coordinate model has to be applied. In the framework of this model, the total energy of the system is described as a sum of the impurity electron energy and impurity-ligand elastic energy, represented by a so-called effective phonon. Such an approach was successfully applied to a number of systems like Cr in the family of II-VI semiconductors or In in CdF_2.[42,43]

Figure 7 shows a configuration diagram representing Mn-related optical transitions in GaN. The photoionization of A^0 to the GaN valence band, observed for highly resistive GaN: Mn,Mg, occurs at the $A^0 + e_{VB}$ equilibrium configuration coordinate Q_1 with optical energy E_{opt}^{VB}. Then the lattice relaxes nonradiatively from Q_1 to $Mn^{2+}(d^5)$ equilibrium coordinate Q_2. The photoionization of $Mn^{2+}(d^5)$, as observed for n-type GaN:Mn samples, occurs with optical energy E_{opt}^{CB} at the Q_2 coordinate.

The photoionization cross section as a function of absorbed photon energy $\sigma(E)$ is given, in the framework of the configuration-coordinate model, by convolution of the pure electron cross section $\sigma_{el}(E)$ and Gaussian broadening:[44–46]

$$\sigma(E) = \frac{1}{2\pi}\int_{(E_{opt}-E)/\Gamma}^{\infty} dz\, e^{-z^2} \sigma_{el}(E_{opt}, E+\Gamma z)\left(1+\frac{\Gamma z}{E}\right), \qquad (4)$$

where Γ is a broadening parameter given by the expression

$$\Gamma = \frac{\hbar\omega_{exc}}{\hbar\omega_0}\sqrt{2E_{rel}\hbar\omega_0 \coth\frac{\hbar\omega_0}{2kT}}. \qquad (5)$$

Here $\hbar\omega_0$ and $\hbar\omega_{exc}$ are vibronic energies in the ground and excited states, respectively, T is the temperature, and k is Boltzmann's constant. The $\sigma(E)$ has thus a shape of a pure
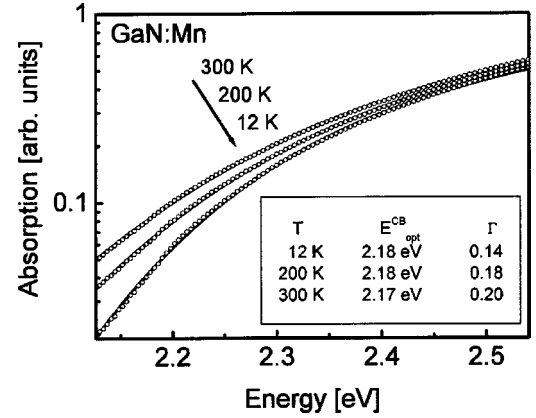
FIG. 8. $Mn^{2+}(d^5)$ photoionization band measured at the temperatures $T = 12-300$ K for a n-type GaN:Mn sample. The solid line represents a fit of the $\sigma(E)$ formula with best fit parameters listed in a table.

electron cross section $\sigma_{el}(E)$, but is Gaussialy broadened near $E = E_{opt}$ due to the interaction with lattice vibrations. The broadening is more evident at higher temperatures.

Figure 8 presents the $Mn^{2+}(d^5)$ photoionization band observed for a GaN:Mn sample measured at temperatures between 12 K and 300 K. The solid line represents the fit of the $\sigma(E)$ formula with the assumed electronic cross section in the form[44,46]

$$\sigma_{el}(E_{opt}, E) \sim \frac{(E - E_{opt})^{3/2}}{E^3}. \qquad (6)$$

The parameters providing the best fit for the spectrum recorded at 300 K are $E_{opt}^{CB} = 2.17 \pm 0.05$ eV and $\Gamma = 0.20 \pm 0.05$ (see the table in Fig. 8). The value of Γ typically grows with impurity-ligand bond ionicity, from 0.13 for CdTe:Cr up to 0.28 for CdF_2:In (Refs. 42 and 43); thus, Γ obtained by us for GaN:Mn is of a very reasonable magnitude.

From the temperature dependence of broadening parameter Γ, assuming $\hbar\omega_{exc}/\hbar\omega_0 = 1$, the relaxation energy and effective phonon may be determined as $E_{rel} = 0.38 \pm 0.05$ eV and $\hbar\omega_0 = 26 \pm 5$ meV, respectively. It is interesting to note that the determined value of $\hbar\omega_0$ is close to the expected energy of Mn local vibration modes (LVM's) in GaN. For comparison, the energy of Mn LVM's determined from infrared absorption spectra in CdTe:Mn equals 23.7 meV, in CdSe 27.5 meV.[47]

The determined relaxation energy agrees reasonably with the value obtained by a rough estimation of absorption onsets, described at the beginning of this section. This fact supports the proposed assignment of the recorded absorption bands to appropriate photoionization transitions of Mn.

By subtracting the relaxation energy ($E_{rel} = 0.38$ eV) from the optical ionization energy ($E_{opt}^{CB} = 2.17$ eV) we may now determine the thermal energy for photoionization of $Mn^{2+}(d^5)$ to the GaN conduction band as equal to $E_{th} = 1.79$ eV. This value determines the location of the Mn acceptor level $A^{0/-}$ with respect to the GaN conduction band.

A similar quantitative analysis of the A^0 photoionization band observed for GaN:Mn,Mg samples is not possible, due to the strong background on which the band is superimposed. The presence of the background makes the fitting procedure unreliable.

The configuration diagram presented in Fig. 7 clearly shows that the $Mn^{2+}(d^5)$ configuration parabola lies inside the $A^0 + e_{VB}$ parabola, and thus no configuration barrier exists. Thus metastability of photostimulated $Mn^{2+}(d^5)$ observed in the photo-EPR experiment for GaN:Mn,Mg must be of the other origin—e.g., due to a Mg trap. The photoexcited holes in the GaN valence band may be trapped to negatively charged Mg acceptors and, in that way, are unable to recombine. The binding energy of the Mg acceptor in GaN equals 250 meV,[48] which corresponds reasonably to the 0.3 eV barrier determined in the photo-EPR experiment.

VI. CONCLUSIONS

The results of studies performed for bulk GaN crystals doped with Mn are consistent with a model localizing the Mn acceptor level deep within the GaN band gap. We have shown that in n-type samples Mn stays unambiguously as an ionized acceptor $Mn^{2+}(d^5)$, while in highly resistive GaN:Mn,Mg crystals Mn is in a lower-charge state, most probably in a neutral-A^0 configuration. From the absorption spectra and configuration-coordinate model analysis we determine the thermal ionization energy of $Mn^{2+}(d^5)$ to the GaN conduction band, thus localization of the $A^{-/0}$ acceptor level below the GaN conduction band, as equal to 1.8 ± 0.1 eV.

Manganese-doped GaN crystals show different magnetic properties, depending on the location of the Fermi level, and thus a configuration of the Mn center. In n-type crystals the magnetization is isotropic Brillouin like, originating from localized Mn spin $S = 5/2$. In highly resistive samples the magnetization shows anisotropy, indicating a nonspherical configuration of Mn.

The nature of the neutral Mn in GaN still needs to be investigated. The basic problem here is localization of an extra hole, on the Mn d shell $[Mn^{3+}(d^4)$ center] or on a delocalized orbit [hydrogenlike $Mn^{2+}(d^5) +$ hole configuration]. To solve this problem further experiments are required, as well as a detailed analysis of the infrared band observed for GaN:Mn,Mg samples, as the band is most probably a fingerprint of the A^0 configuration of Mn in GaN.

[1] T. Dietl, H. Ohno, F. Matsukura, J. Cibert, and D. Ferrand, Science **287**, 1019 (2000).

[2] N. Theodoropoulou, A. F. Hebard, M. E. Overberg, C. R. Abernathy, S. J. Pearton, S. N. G. Chu, and R. G. Wilson, Appl. Phys. Lett. **78**, 3475 (2001).

[3] M. E. Overberg, C. R. Abernathy, S. J. Pearton, N. A. Theodoropoulou, K. T. McCarthy, and A. F. Hebard, Appl. Phys. Lett. **79**, 1312 (2001).

[4] M. L. Reed, N. A. El-Masry, H. H. Stadelmaier, M. K. Ritums, M. J. Reed, C. A. Parker, J. C. Roberts, and S. M. Bedair, Appl. Phys. Lett. **79**, 3473 (2001).

[5] Y. L. Soo, G. Kioseoglou, S. Kim, S. Huang, Y. H. Kao, S. Kuwabara, S. Owa, T. Kondo, and H. Munekata, Appl. Phys. Lett. **79**, 3926 (2001).

[6] T. Sasaki, S. Sonoda, Y. Yamamoto, K. Suga, S. Shimizu, K. Kindo, and H. Hori, J. Appl. Phys. **91**, 7911 (2002).

[7] M. Zajac, R. Doradzinski, J. Gosk, J. Szczytko, M. Lefeld-Sosnowska, M. Kaminska, A. Twardowski, M. Palczewska, E. Grzanka, and W. Gebicki, Appl. Phys. Lett. **78**, 1276 (2001).

[8] M. Zajac, J. Gosk, M. Kaminska, A. Twardowski, T. Szyszko, and S. Podsiadlo, Appl. Phys. Lett. **79**, 2432 (2001).

[9] A. Wolos, M. Zajac, J. Gosk, M. Palczewska, M. Kaminska, A. Twardowski, M. Bockowski, I. Grzegory, and S. Porowski, in *Proceedings of the 26th International Conference on the Physics of Semiconductors, Edinburgh, 2002*, edited by A. R. Long and J. H. Davies (Institute of Physics, Bristol, 2002), p. D44.

[10] M. Zajac, J. Gosk, E. Grzanka, M. Kaminska, A. Twardowski, B. Strojek, T. Szyszko, and S. Podsiadlo, J. Appl. Phys. **93**, 4715 (2003).

[11] C. Y. Fong, V. A. Gubanov, and C. Boekema, J. Electron. Mater. **29**, 1067 (2000).

[12] K. Sato and H. Katayama-Yoshida, Jpn. J. Appl. Phys., Part 2 **40**, L485 (2001).

[13] H. Katayama-Yoshida, R. Kato, and T. Yamamoto, J. Cryst. Growth **231**, 428 (2001).

[14] M. van Schilfgaarde and O. N. Mryasov, Phys. Rev. B **63**, 233205 (2001).

[15] E. Kulatov, H. Nakayama, H. Mariette, H. Ohta, and Yu. A. Uspenskii, Phys. Rev. B **66**, 045203 (2002).

[16] L. Kronik, M. Jain, and J. R. Chelikowsky, Phys. Rev. B **66**, 041203(R) (2002).

[17] T. Dietl, F. Matsukura, and H. Ohno, Phys. Rev. B **66**, 033203 (2002).

[18] T. Dietl, Phys. Status Solidi B **240**, 433 (2003).

[19] N. Almeleh and B. Goldstein, Phys. Rev. **128**, 1568 (1962).

[20] J. Szczytko, A. Twardowski, K. Swiatek, M. Palczewska, M. Tanaka, T. Hayashi, and K. Ando, Phys. Rev. B **60**, 8304 (1999).

[21] J. Kreissl, W. Ulrici, M. El-Metoui, A. M. Vasson, A. Vasson, and A. Gavaix, Phys. Rev. B **54**, 10 508 (1996).

[22] J. Schneider, U. Kaufmann, W. Wilkening, M. Baeumler, and F. Kohl, Phys. Rev. Lett. **59**, 240 (1987).

[23] R. A. Chapman and W. G. Hutchinson, Phys. Rev. Lett. **18**, 443 (1967).

[24] A. Baldereschi and N. O. Lipari, Phys. Rev. B **8**, 2697 (1973).

[25] B. Lambert, B. Clerjaud, C. Naud, B. Deveaud, G. Picoli, and Y. Toudic, in *Proceedings of the Thirteenth International Conference on Defects in Semiconductors*, edited by L. K. Kimerling

and J. M. Parsey (Metallic Society, AIME, Warrendale, PA, 1985), p. 1141.

[26] M. J. Caldas, A. Fazzio, and A. Zunger, Appl. Phys. Lett. **45**, 671 (1984).

[27] J. M. Langer, C. Delerue, M. Lannoo, and H. Heinrich, Phys. Rev. B **38**, 7723 (1988).

[28] G. Martin, S. Strite, J. Thornton, and H. Morkoc, Appl. Phys. Lett. **58**, 2375 (1991).

[29] R. Y. Korotkov, J. M. Gregie, and B. W. Wessels, Physica B **308–310**, 30 (2001).

[30] T. Graf, M. Gjukic, M. S. Brandt, M. Stutzmann, and O. Ambacher, Appl. Phys. Lett. **81**, 5159 (2002).

[31] T. Graf, M. Gjukic, M. Hermann, M. S. Brandt, M. Stutzmann, L. Gorgens, J. B. Philipp, and O. Ambacher, J. Appl. Phys. **93**, 9697 (2003).

[32] S. Krukowski, M. Bockowski, B. Lucznik, I. Grzegory, S. Porowski, T. Suski, and Z. Romanowski, J. Phys.: Condens. Matter **13**, 8881 (2001).

[33] B. Clerjaud, D. Cote, C. Naud, R. Bouanani-Rahbi, D. Wasik, K. Pakula, J. M. Baranowski, T. Suski, E. Litwin-Staszewska, M. Bockowski, and I. Grzegory, Physica B **308–310**, 117 (2001).

[34] P. G. Baranov, I. V. Ilyin, E. N. Mokhov, and A. D. Roenkov, Semicond. Sci. Technol. **11**, 1843 (1996).

[35] T. Graf, M. Gjukic, M. Hermann, M. S. Brandt, M. Stutzmann, and O. Ambacher, Phys. Rev. B **67**, 165215 (2003).

[36] Ch. P. Poole, *Electron Spin Resonance: A Comprehensive Treatise on Experimental Techniques* (Wiley, New York, 1967), p. 695.

[37] W. Gotz, N. M. Johnson, and D. P. Bour, Appl. Phys. Lett. **68**, 3470 (1996).

[38] M. Herbich, W. Mac, A. Twardowski, and M. Demianiuk, Phys. Rev. B **59**, 2726 (1999).

[39] M. Herbich, W. Mac, A. Twardowski, K. Ando, Y. Shapira, and M. Demianiuk, Phys. Rev. B **58**, 1912 (1998).

[40] A. M. Stoneham, *Theory of Defects in Solids* (Oxford University Press, New York, 1975), p. 271.

[41] B. Clerjaud, J. Phys. C **18**, 3615 (1985) and references therein.

[42] M. Kaminska, J. Baranowski, and M. Godlewski, Inst. Phys. Conf. Ser. **43**, 303 (1979).

[43] U. Piekara, J. M. Langer, and B. Krukowska-Fulde, Solid State Commun. **23**, 583 (1977).

[44] G. Lucovsky, Solid State Commun. **3**, 299 (1965).

[45] M. Jaros, Solid State Phys. **8**, L264 (1975).

[46] A. A. Kopylov and A. N. Pikhtin, Fiz. Tverd. Tela (Leningrad) **16**, 1837 (1974).

[47] A. J. Mayur, M. D. Sciacca, H. Kim, I. Miotkowski, A. K. Ramdas, S. Rodriguez, and G. C. La Rocca, Phys. Rev. B **53**, 12 884 (1996).

[48] S. C. Strite, in *Properties of Group III Nitrides*, edited by J. H. Edgar (INSPEC, London, 1994), p. 272.